Organometallics **2000,** *19,* 5149−5154

Skeletal Growth by Condensation of Small Metal Fragments on a Carbido Carbonyl Cluster. Synthesis of the Anions $[Rh_{15}C_2(CO)_{24}X_2]^{3-}$ (X = Cl, Br, I) and Molecular Structure of the Bromo and Iodo Derivatives

Alessandro Fumagalli,*,† Secondo Martinengo,‡,§ Giovanni Bernasconi,§ Luciana Noziglia,§ Vincenzo G. Albano,‖,⊥ Magda Monari,⊥ and Carlo Castellari⊥

Dipartimento di Biologia Strutturale e Funzionale dell'Università degli Studi dell'Insubria, Via J. H. Dunant 3, 21100 Varese, Italy, Dipartimento di Chimica Inorganica, Metallorganica e Analitica dell'Università e Centro di Studio CNR sulla Sintesi e la Struttura dei Composti dei Metalli di Transizione nei Bassi Stati di Ossidazione, Via G. Venezian 21, 20133 Milano, Italy, and Dipartimento di Chimica "G. Ciamician" dell'Università degli Studi di Bologna, Via Selmi 2, 40126 Bologna, Italy

Received July 5, 2000

The reaction of $[Rh_{12}C_2(CO)_{24}]^{2-}$ (as K^+ salt) with Rh^I derivatives yields an uncharacterized intermediate (**1**) from which, by reaction with halides, the new carbido-carbonyl cluster anions $[Rh_{15}C_2(CO)_{24}X_2]^{3-}$ (X = Cl, **2a**; Br, **2b**; I, **2c**) have been obtained. The molecular structures of **2b** and **2c** as $[N(n\text{-}Pr)_4]^+$and $[NEt_4]^+$ salts, respectively, have been determined by single-crystal X-ray diffractometry. The two anions are isostructural and contain a $Rh_{15}C_2$ cluster that can be described as a C_{2v} centered and tetracapped pentagonal prism. The carbide atoms occupy octahedral interstices, and the halide ligands span basal edges of the prism. The CO ligands have been found partially ordered in the dibromo derivative and totally ordered in the diiodo one, adopting an unprecedented and peculiar asymmetric stereogeometry. The room-temperature solution ^{13}C NMR spectrum indicates that in compound **2c** a fraction of the carbonyl ligands is fluxional, probably those found disordered in the solid state structure of **2b**.

Introduction

The buildup mechanism leading to high nuclearity metal carbonyl clusters is a complex sequence of steps which, in a simplified vision, can be postulated as occurring through two limiting processes: (i) the condensation of mononuclear or small polynuclear fragments around a nucleus (as much as in crystal growth), (ii) the assembling of polyatomic units (M_n) to give multiple nuclearities (M_{xn}, $x = 2, 3$, etc.). The processes of the first type are by far the most recurrent and include the pyrolytic reactions.[1] Here the decarbonylation process, in which M−CO bonds are broken, is generally accompanied by a more or less extensive skeletal disruption with formation of small metallic fragments, which, eventually, condense on a nucleus. The interstitial presence of main group atoms (C, N) strengthens the metal atom skeleton and somewhat prevents the cluster breakdown, thus favoring processes of the second kind. As a result, generally within the temperature range 50−100 °C, only decarbonylation is observed, often with formation of unsaturated units that undergo condensation processes.[2,3] The process that yields $[Rh_{12}C_2(CO)_{24}]^{2-}$,[4] from $[Rh_6C(CO)_{15}]^{2-}$,[5] is very likely of the second kind. In our studies on cluster expansion we have chosen to try reactions of the first kind but at low temperature, to preserve the integrity of the condensation nucleus, and this requires the introduction of small specific fragments. The dianion $[Rh_{12}C_2(CO)_{24}]^{2-}$ appeared as an ideal substrate because it is robust enough to withstand temperatures up to 60−80 °C without fragmentation (although skeletal rearrangements around the pivotal carbides may not be ruled out) and its relatively low anionic charge allows predictable redox condensations[6] of cationic and even anionic metal fragments (such as $[Rh(CO)_4]^-$). Moreover, its potassium salt is relatively easy to produce in several gram amounts. The "bricks" we have used are mono- or binuclear species, such as $[Rh(CO)_2(MeCN)_2]^+$, $[Rh(CO)_2Cl_2]^-$, and $[Rh(CO)_2Cl]_2$, and also small clusters that can be easily fragmented, such as

---

* For correspondence on synthesis and chemical characterization.

† Università degli Studi dell'Insubria.

‡ Deceased on August 1, 1999.

§ Università e Centro di Studio CNR sulla Sintesi e la Struttura dei Composti dei Metalli di Transizione nei Bassi Stati di Ossidazione.

‖ For correspondence on structural characterization.

⊥ Università degli Studi di Bologna.

(1) Chini, P.; Heaton, B. T. *Top. Curr. Chem.* **1977**, *71*, 8.

(2) Fumagalli, A.; Della Pergola, R. In *Metal Clusters in Chemistry*; Braunstein, P., Oro, L. A., Raithby, P. R., Eds.; Wiley−VCH: New York, 1999; pp334−335.

(3) A mechanism of this kind has been proved in the synthesis of the nitrido cluster $[Rh_{28}N_4(CO)_{41}H_x]^{4-}$ from $[Rh_{14}N_2(CO)_{25}]^{2-}$. Fumagalli, A.; Martinengo S.; Bernasconi, G.; Ciani, G.; Proserpio, D. M.; Sironi, A. *J. Am. Chem. Soc.* **1997**, *119*, 1450.

(4) Albano, V. G.; Braga, D.; Chini, P.; Strumolo, D.; Martinengo, S. *J. Chem. Soc., Dalton Trans.* **1983**, 249.

(5) Albano, V. G.; Chini, P.; Martinengo, S.; McCaffrey, D. J. A.; Strumolo, D.; Heaton, B. T. *J. Am. Chem. Soc.* **1974**, *96*, 8106.

(6) A definition of redox condensations as "reactions between coordinatively saturated species in different oxidation state" was given by: Chini, P.; Longoni, G.; Albano, V. G. *Adv. Organomet. Chem.* **1976**, *14*, 313.

10.1021/om000577p CCC: $19.00
Publication on Web 10/31/2000

$[Rh_4(CO)_{12}]$ in the presence of halides. The first results of this investigation are here reported.

Results and Discussion

Synthesis and Chemical Characterization. The reaction of the anion $[Rh_{12}C_2(CO)_{24}]^{2-}$ [4] (as potassium salt) with $[Rh(CO)_2(MeCN)_2]BF_4$[7] (1.5−2 moles per mole of the dicarbide) is solvent dependent. While in MeCN no reaction is observed, in THF or CH_2Cl_2 there is prompt formation of a product with a characteristic IR spectrum (THF: 2082w, 2050s, 1874m, 1830mw; CH_2Cl_2: 2092w, 2054s, 1875m, 1837mw). The high value of the main terminal CO stretching is consistent with a low specific anionic charge, as expected for a giant mono- or dianion. In any case this step, not even observable in methanol or acetone, is only the beginning of a reaction sequence slowly evolving toward equilibrium. As monitored by IR spectroscopy, after several days at room temperature, or a few hours at 60−70 °C, anion **1** (with characteristic IR stretchings at ca. 2034 and 1860−50 cm^{-1}) is eventually obtained as the main product. The presence of chloride ions, an impurity often present in $K_2[Rh_{12}C_2(CO)_{24}]$, severely hinders the reaction, due to consumption of $[Rh(CO)_2(MeCN)_2]^+$ with formation of the apparently inert $[Rh(CO)_2Cl_2]^-$. However, anion **1** can also be obtained by reaction of the carbide with 1.2−1.5 mol of $[Rh(CO)_2Cl]_2$, an amount of Rh^I twice that of $[Rh(CO)_2(MeCN)_2]^+$. This is consistent with the formation of the unreactive $[Rh(CO)_2Cl_2]^-$, according to eq 1.

$$[Rh_{12}C_2(CO)_{24}]^{2-} + 1.2{-}1.5\ [Rh(CO)_2Cl]_2 \rightarrow \mathbf{1} + [Rh(CO)_2Cl_2]^- \quad (1)$$

After several attempts, we have optimized the molar ratio of the reactants only within a range. This uncertainty derives from the purity of the substrate, which can be different from sample to sample and is formulated in the range $K_2[Rh_{12}C_2(CO)_{24}]\cdot 2{-}4thf$. Moreover it reflects the nonstoichiometric nature of the reaction because it takes place through several sequential steps and perhaps parallel paths. The relatively high IR stretching of the terminal CO's in **1** indicates a low specific charge on the cluster anion. This makes it reactive toward nucleophilic reagents, and in fact, though indefinitely stable in the solution where synthesized, the anion easily reacts with halides and bases in general. Decomposition can be observed even on changing the solvent to MeCN, very likely through the extraction of $[Rh(CO)_2(MeCN)_2]^+$ fragments, with formation of a more reduced species (IR stretchings at 2010s, 1853m, 1807mw cm^{-1}) different from the original $[Rh_{12}C_2(CO)_{24}]^{2-}$, perhaps proof that any relation to the original carbide has become lost in **1**. Due to this particular reactivity, the isolation of the anion **1** by metathesis of its potassium salt can be done only with $[BF_4]^-$ or $[PF_6]^-$ salts of bulky cations; crown ethers have also been used. Among the many attempts done, only the $[NEt_4]^+$, $[NBu_4]^+$, and [K(18-crown-6)]$^+$ salts gave precipitates containing a few sparse crystals. Unfortunately none has been found suitable for X-ray structural investigations and recrystallization has led to decomposition. Elemental analyses have not been of much help, due to the low purity of the samples.

Scheme 1

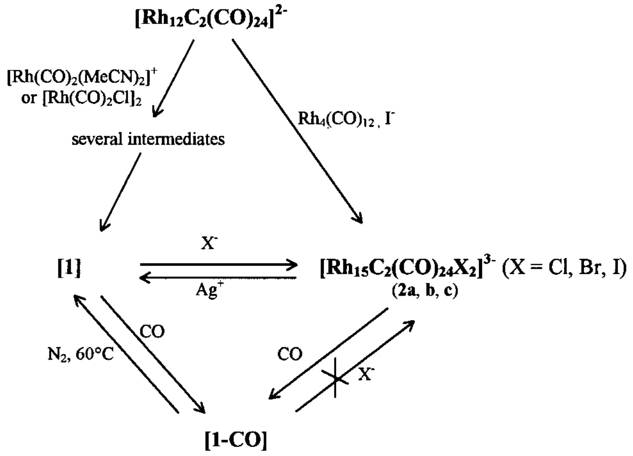

The role of the elusive anion **1** is reported in Scheme 1, where its remarkable reactivity toward carbon monoxide is also evidenced. Acetone or THF solutions exposed at room temperature to CO (ca. 100 kPa), after 0.5−1 h stirring to favor equilibration, show a modification of the IR pattern, essentially in the bridging CO region (Table 1), where a medium-weak band at ca. 1820 cm^{-1} moves to 1830−40 cm^{-1} and broadens. This new species (**1-CO**) is very likely formed by addition of one or more CO's. Stable under nitrogen, it regenerates the starting product after some heating (2 h, 60 °C). Any attempt to isolate **1-CO** failed.

The reaction of **1** with halides (eq 2) gives the whole series of dihalogeno derivatives:

$$\mathbf{1} + X^- \text{ (excess)} \rightarrow [Rh_{15}C_2(CO)_{24}X_2]^{3-} \quad [X = Cl\ (\mathbf{2a}),\ Br\ (\mathbf{2b}),\ I\ (\mathbf{2c})] \quad (2)$$

When the anion **1** (as potassium salt in methanol) is treated dropwise with a propan-2-ol solution of a tetraalkylammonium halide, the respective halogeno derivative is formed and, upon addition of excess cation, the bulky cation salt is eventually recovered by precipitation. All three anions were isolated as pure compounds with a suitable cation, but only **2b** and **2c** have given crystals suitable for X-ray diffraction experiments and have been structurally characterized (see later). Remarkably, the three halides do not react under a CO atmosphere (ca. 100 kPa) where the anion **1-CO** is produced, and even an excess of $[N(n\text{-}Pr)_4]Br$ in precipitating conditions is ineffective.

Particularly interesting is the observation made after an attempt to produce the dibromo derivative: quick addition of excess $[NEt_4]Br$ in water gave immediate precipitation of still unreacted anion **1** (as $[NEt_4]^+$ salt) with only minor amounts of the trianion $[Rh_{15}C_2(CO)_{24}Br_2]^{3-}$ and no evidence of the expected intermediate monobromo dianion (see later). This suggests that the monohalo derivative is more reactive than **1** toward further halide addition. It is also worth noting that $[SCN]^-$ behaves differently from the three halides; its reaction with **1** gives a product whose IR spectrum (K^+ salt in MeOH: 2078 w, 2022 s, 1850 m, 1803 mw cm^{-1}) indicates a lower specific charge, possibly consistent with a somewhat related monothiocyanato dianion

---

[7] Albano, V. G.; Chini, P.; Martinengo, S.; Sansoni, M.; Strumolo, D. *J. Chem. Soc., Chem. Commun.* **1974**, 299.

Table 1. IR Data[a]

anion	cat (solv)	CO stretchings
1	K^+ (MeOH)	2062 w, 2035 s, 1859 m, 1819 mw
	K^+ (thf)	2063 w, 2033 s, 1852 m, 1827 sh
	$[NPr_4]^+$ (acetone)	2050 w, 2034 s, 1912w, 1856 ms, 1845 sh, 1815 m
1-CO	K^+ (MeOH)	2069 w, 2036 s, 1855 ms, 1832 m
	K^+ (thf)	2067 w, 2033 s, 1852 ms, 1840−30 m (brd)
	$[NPr_4]^+$ (acetone)	2086 w, 2035 s, 1963 w, 1854 ms, 1828 m
$[Rh_{15}C_2(CO)_{24}Cl_2]^{3-}$	$[NMe_4]^+$ (acetone)	2040 m, 2011 s, 1968 m, 1873 mw, 1841 ms, 1830 sh, 1802 m
	$[NEt_4]^+$ (acetone)	2039 m, 2011 s, 1968 m, 1874 mw, 1841 ms, 1828 sh, 1799 m
	$[NEt_4]^+$ (MeCN)	2043 m, 2013 s, 1978 m, 1873 mw, 1840 ms, 1829 sh, 1797 m
$[Rh_{15}C_2(CO)_{24}Br_2]^{3-}$	$[NPr_4]^+$ (acetone)	2039 m, 2011 s, 1977 m, 1874 mw, 1841 ms, 1828 sh, 1798 m
	$[NEt_4]^+$ (acetone)	2038 m, 2010 s, 1967 m, 1872 mw, 1841 ms, 1827 sh, ca. 1800 m
$[Rh_{15}C_2(CO)_{24}I_2]^{3-}$	$[NEt_4]^+$ (MeCN)	2041 m, 2013 s, 1975 m, 1869 mw, 1838 ms, 1825 sh, 1792 m
	$[NEt_4]^+$ (acetone)	2038 m, 2010 s, 1967 mw, 1871 w, 1840 ms, 1827 sh, 1795 m
	$[NMe_4]^+$ (acetone)	2038 m, 2010 s, 1967 mw, 1871 w, 1840 ms, 1830 sh, 1794 m
	$[NMe_4]^+$ (thf)	2039 m, 2011 s, 1972 m, 1875 mw, 1833 ms, 1810−1790 sh

[a] Wavenumbers are in cm^{-1} (±2); s = strong, m = medium, w = weak, sh = shoulder.

$[Rh_{15}C_2(CO)_x(SCN)]^{2-}$. The latter product has not been further investigated.

An alternative and convenient one-pot synthesis of $[Rh_{15}C_2(CO)_{24}I_2]^{3-}$ has been developed, according to the optimized stoichiometry (eq 3):

$$[Rh_{12}C_2(CO)_{24}]^{2-} + Rh_4(CO)_{12} + 2I^- \xrightarrow{\text{THF, 60 °C}} [Rh_{15}C_2(CO)_{24}I_2]^{3-} \quad (3)$$

Here, the reaction of $Rh_4(CO)_{12}$ with sodium or tetraalkylammonium ($[NMe_4]^+$, $[NEt_4]^+$) iodide[8] yields in situ the fragments that condense on the dicarbide, to give the anion **2c** in good yields. The $[NEt_4]^+$ salt of **2c** has been characterized by X-ray diffraction (see further on). The same reaction, using $[NPr_4]Br$, yields the dibromo derivative.

Trianions **2b** and **2c** react with $AgBF_4$ or $TlPF_6$ in acetone solution to give the common precursor **1** according to eq 4:

$$[Rh_{15}C_2(CO)_{24}X_2]^{3-} + 2\,AgBF_4 \rightarrow \mathbf{1} + 2\,AgX\downarrow + 2\,[BF_4]^- \ (X = Br, I) \quad (4)$$

This reaction suggests a close structural relationship between the precursor and the two halogeno derivatives.

By addition of just 1 mol (per mole) of $AgBF_4$, the diiodo compound gives evidence of an intermediate product whose IR pattern retains the shape and relative intensity of the bands of $[Rh_{15}C_2(CO)_{24}I_2]^{3-}$, but shifted to higher wavenumbers by ca. 15 cm^{-1} ($[NEt_4]^+$ salt in acetone: 2025 s, 1989 m, 1894 w, 1853 ms, 1810 m cm^{-1}). Very likely this is the dianionic monoiodo derivative.

Also CO is able to induce halide displacement; thus $[Rh_{15}C_2(CO)_{24}Br_2]^{3-}$ in THF solution slowly reacts (1−2 days) with CO (ca. 100 kPa), yielding **1-CO**. The diiodo derivative, upon prolonged exposure to CO (2−3 days), gives evidence of further reaction with formation of a mixture of at least two unidentified products.

Finally, with reference to the reactions of Scheme 1, we are led to think of anion **1** as an “unsaturated” species able to add, in competition, halide or carbonyl ligands in an equilibrium depending on the nature of X^- and, likely, the partial pressure of CO. This would fit for **1** being a monoanion with formula $[Rh_{15}C_2(CO)_x]^-$, possibly with a metal atom skeleton similar to that found in **2b** and **2c**. The anion $[Rh_{15}C_2(CO)_{28}]^-$ (**3**),[9] obtained several years ago, has indeed a metal atom cluster very similar to that of the trianionic halogeno derivatives (see later), but it is not their precursor. Anion **3**, originally obtained by oxidation of $[Rh_6C(CO)_{15}]^{2-}$ with Fe^{3+} in water, directly precipitates as crystalline hydronium salt. An attempt to prepare **2b** by reaction of **3** with $[NPr_4]Br$, as well as the acidification of a solution of **1** to possibly precipitate the $(H_3O)^+$ salt of **3**, has been unsuccessful. Even the IR spectra of **3** and **1** in acetone (this latter as K^+ salt) do not bear any resemblance.

Spectroscopic Measurements. The infrared spectra (CO stretching region) of anions **1**, **1-CO**, **2a**, **2b**, and **2c** with several cations and in various solvents are reported in Table 1. The similarity of the three halo derivatives' spectra is quite evident and supports an identical structure of the anions in solution.

A natural abundance ^{13}C NMR spectrum of $[NEt_4]_3[Rh_{15}C_2(CO)_{24}I_2]$ (**2c**) has been obtained in CD_3CN solution at room temperature. In the carbonyl region (185−235 ppm), two doublets, clearly terminally bonded carbonyls, have been found at 187.5 ppm ($J_{Rh-C} = 87.7$ Hz) and 199.1 ppm ($J_{Rh-C} = 95.8$ Hz). By integration they correspond to 2 + 2 equivalent carbonyls. In the bridging region, a triplet at 222.8 ppm ($J \approx 40$ Hz), and a doublet of doublets (asymmetric bridges) at 231.4 ppm ($J = 34.8$ Hz, $J = 53.8$ Hz) integrate to, respectively, ca. 4 and 3 ligands. The remaining carbonyls (ca. 13) give a single broad resonance in the intermediate region at 208.9 ppm, consistent with fluxionality on a limited region of the metal skeleton, probably the same region that in the solid state structure exhibits an asymmetric ligand disposition and is affected by disorder in the dibromo derivative (see next section). The resonance due to the two carbido atoms has also been detected as a complex multiplet at 388 ppm. This value, as expected at low field, is significantly different from the values found for other compounds containing carbon atoms in octahedral cages, as in the case of $[Rh_6C(CO)_{13}]^{2-}$ (470.0 ppm),[10] $[HRh_6C(CO)_{13}]^-$ (460.4 ppm),[11] and $[Rh_6C(CO)_{13}\{Au_2(PPh_3)_2\}]$ (452.5 ppm).[12]

X-ray Molecular Structures of the Trianions $[Rh_{15}C_2(CO)_{24}X_2]^{3-}$ (X = Br (2b), I (2c)). The structure

---

[8] Fumagalli, A.; Martinengo, S.; Galli, D.; Allevi, C.; Ciani, G.;. Sironi, A. *Inorg. Chem.* **1990**, *29*, 1408.

[9] Albano, V. G.; Sansoni, M.; Chini, P.; Martinengo, S.; Strumolo, D. *J. Chem. Soc., Dalton Trans.* **1976**, 970.

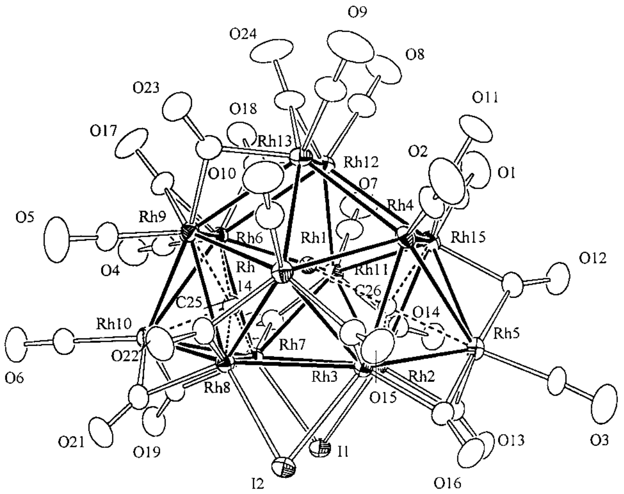

Figure 1. Structure of the $[Rh_{15}C_2(CO)_{24}I_2]^{3-}$ anion (C_1 symmetry of the CO ligands' stereogeometry on the C_{2v} metal atom cluster). The carbonyl carbon atoms are numbered in accord with the corresponding oxygen atoms.

of the $[N(n\text{-}Pr)_4]^+$ salt of the dibromo derivative (**2b**) was studied first, but its molecular geometry was ascertained only in part because a relevant number of CO ligands were found disordered and, despite repeated efforts, it was not possible to produce a complete molecular model.[13]

As soon as good crystals of the diiodo derivative (**2c**) as $[NEt_4]^+$ salt were grown, an X-ray diffraction experiment was undertaken and a detailed molecular model was eventually obtained. Hereafter we describe and discuss the structure of **2c** and rationalize the disorder affecting **2b**.

Table 2. Selected Bond Lengths (Å) for $[NEt_4]_3[Rh_{15}C_2(CO)_{24}I_2]$ (2c)

Rh(2)−Rh(15)	3.038(1)	Rh(3)−I(2)	2.687(1)
Rh(4)−Rh(15)	2.722(1)	Rh(8)−I(2)	2.670(1)
Rh(5)−Rh(15)	2.880(1)	Rh(1)−C(25)	1.923(4)
Rh(1)−Rh(15)	2.910(1)	Rh(6)−C(25)	2.181(4)
Rh(11)−Rh(15)	3.002(1)	Rh(7)−C(25)	1.998(4)
Rh(12)−Rh(15)	3.021(1)	Rh(8)−C(25)	2.003(4)
Rh(2)−Rh(5)	2.740(1)	Rh(9)−C(25)	2.218(4)
Rh(2)−Rh(11)	2.807(1)	Rh(10)−C(25)	2.083(4)
Rh(2)−Rh(7)	2.892(1)	Rh(1)−C(26)	1.976(4)
Rh(2)−Rh(1)	3.008(1)	Rh(2)−C(26)	2.059(4)
Rh(2)−Rh(3)	3.037(1)	Rh(3)−C(26)	1.995(4)
Rh(3)−Rh(5)	2.760(1)	Rh(4)−C(26)	2.109(4)
Rh(3)−Rh(14)	2.839(1)	Rh(5)−C(26)	2.123(4)
Rh(3)−Rh(4)	2.870(1)	Rh(15)−C(26)	2.116(4)
Rh(3)−Rh(8)	2.962(1)	Rh(15)−C(1)	1.877(5)
Rh(3)−Rh(1)	3.043(1)	C(1)−O(1)	1.138(6)
Rh(4)−Rh(1)	2.794(1)	Rh(4)−C(2)	1.870(5)
Rh(4)−Rh(13)	2.816(1)	C(2)−O(2)	1.138(6)
Rh(4)−Rh(14)	2.877(1)	Rh(5)−C(3)	1.909(5)
Rh(4)−Rh(5)	3.121(1)	C(3)−O(3)	1.124(6)
Rh(6)−Rh(1)	2.805(1)	Rh(6)−C(4)	1.887(5)
Rh(6)−Rh(9)	2.805(1)	C(4)−O(4)	1.131(5)
Rh(6)−Rh(7)	2.889(1)	Rh(9)−C(5)	1.876(6)
Rh(6)−Rh(12)	2.922(1)	C(5)−O(5)	1.122(6)
Rh(6)−Rh(11)	2.945(1)	Rh(10)−C(6)	1.895(6)
Rh(6)−Rh(10)	3.001(1)	C(6)−O(6)	1.131(6)
Rh(7)−Rh(10)	2.713(1)	Rh(11)−C(7)	1.890(5)
Rh(7)−Rh(11)	2.820(1)	C(7)−O(7)	1.117(5)
Rh(7)−Rh(1)	3.036(1)	Rh(12)−C(8)	1.868(6)
Rh(7)−Rh(8)	3.173(1)	C(8)−O(8)	1.155(6)
Rh(8)−Rh(10)	2.714(1)	Rh(13)−C(9)	1.857(6)
Rh(8)−Rh(14)	2.792(1)	C(9)−O(9)	1.131(6)
Rh(8)−Rh(9)	2.918(1)	Rh(14)−C(10)	1.868(5)
Rh(8)−Rh(1)	3.009(1)	C(10)−O(10)	1.138(6)
Rh(9)−Rh(1)	2.807(1)	Rh(4)−C(11)	1.948(5)
Rh(9)−Rh(13)	2.884(1)	Rh(15)−C(11)	2.112(5)
Rh(9)−Rh(14)	2.935(1)	C(11)−O(11)	1.180(5)
Rh(9)−Rh(10)	3.021(1)	Rh(15)−C(12)	2.068(5)
Rh(11)−Rh(12)	2.842(1)	Rh(5)−C(12)	2.059(5)
Rh(11)−Rh(1)	2.854(1)	C(12)−O(12)	1.162(6)
Rh(12)−Rh(1)	2.694(1)	Rh(2)−C(13)	1.979(5)
Rh(12)−Rh(13)	2.836(1)	Rh(5)−C(13)	2.122(5)
Rh(13)−Rh(1)	2.698(1)	C(13)−O(13)	1.165(5)
Rh(13)−Rh(14)	2.890(1)	Rh(2)−C(14)	2.018(4)
Rh(14)−Rh(1)	2.963(1)	Rh(11)−C(14)	1.993(5)
Rh(2)−I(1)	2.690(1)	C(14)−O(14)	1.183(5)
Rh(7)−I(1)	2.691(1)	Rh(3)−C(15)	2.039(5)
Rh(14)−C(15)	2.007(5)	Rh(11)−C(20)	2.019(5)
C(15)−O(15)	1.166(6)	C(20)−O(20)	1.172(5)
Rh(3)−C(16)	1.939(5)	Rh(8)−C(21)	2.023(5)
Rh(5)−C(16)	2.245(5)	Rh(10)−C(21)	2.053(5)
C(16)−O(16)	1.162(5)	C(21)−O(21)	1.160(5)
Rh(6)−C(17)	2.049(5)	Rh(8)−C(22)	2.047(5)
Rh(9)−C(17)	2.032(5)	Rh(14)−C(22)	2.005(5)
C(17)−O(17)	1.159(5)	C(22)−O(22)	1.168(5)
Rh(6)−C(18)	2.047(5)	Rh(9)−C(23)	2.045(5)
Rh(12)−C(18)	2.010(5)	Rh(13)−C(23)	1.989(5)
C(18)−O(18)	1.174(5)	C(23)−O(23)	1.178(5)
Rh(7)−C(19)	2.016(5)	Rh(12)−C(24)	2.020(5)
Rh(19)−C(19)	2.032(5)	Rh(13)−C(24)	2.002(5)
C(19)−O(19)	1.177(5)	C(24)−O(24)	1.169(6)
Rh(7)−C(20)	2.031(5)		

The structure of $[Rh_{15}C_2(CO)_{24}I_2]^{3-}$ (shown in Figure 1 with relevant bond distances listed in Table 2) features a rare metal atom aggregation and a unique ligand arrangement. The molecular stereochemistry is as follows: (i) The $Rh_{15}C_2$ core can be described as a centered and tetracapped pentagonal prism of C_{2v} idealized symmetry. The four capping Rh atoms are positioned on the pentagonal and two noncontiguous rectangular faces of the pentagonal prism. The latter define two octahedral cavities occupied by the carbide atoms. (ii) The iodide ligands occupy bridging positions on the basal prism edges connecting the octahedral units and can be considered four-electron donors (see later). (iii) The CO ligands are bonded 10 terminally and 14 edge bridging. Twelve ligands covering the lower part of the metal atom polyhedron (with reference to Figure 1) conform to the C_{2v} cluster symmetry: four are terminally bonded to the capping atoms [CO(3), (6), (7), (10)] and two sets of four span edges of the octahedral and pentagonal caps [CO(13), (16), (19), (21) and CO(14), (15), (20), (22), respectively]. The remaining 12 ligands are distributed in an asymmetric way so that the actual symmetry of the anion as a whole is C_1. More precisely the bridging CO(18) and CO(23) do not find corresponding ligands under the C_{2v} symmetry operations; the same can be said for CO(12). It is worth noting that a more regular ligand distribution can be envisaged if only the CO(12) and CO(24) bridging ligands are removed from their actual positions and placed on the edges Rh(13)−Rh(15) and Rh(12)−Rh(14), thus becoming symmetry equivalent of CO(18) and CO(23), respectively. In this way the whole ligand coverage would conform to the full C_{2v} symmetry of the metal atom core (with minor rotational adjustments of the vicinal groups). Therefore the actual asymmetric ligand disposition is not a geometric necessity, and, more than that, it breaks

---

(10) Heaton, B. T.; Strona, L.; Martinengo, S. *J. Organomet. Chem.* **1981**, *215*, 415.

(11) Bordoni, S.; Heaton, B. T.; Seregni, C.; Strona, L.; Goodfellow, R. J.; Hursthouse, M. B.; Thornton-Pett, M.; Martinengo, S. *J. Chem. Soc., Dalton Trans.* **1988**, 2103.

(12) Fumagalli, A.; Martinengo, S.; Albano, V. G.; Braga, D.; Grepioni, F. *J. Chem. Soc., Dalton Trans.* **1989**, 2343.

(13) Crystal data for $[N(n\text{-}Pr)_4]_3[Rh_{15}C_2(CO)_{24}Br_2]$: monoclinic, space group *C*2/*c* (No. 15), $a = 21.8798(8)$, $b = 22.2156(8)$, $c = 17.0870(6)$ Å, $\beta = 93.820(1)$, $Z = 4$, $V = 8287.1(5)$ Å^3, $D_c = 2.372$ Mg m^{-3}, μ(Mo Kα) $= 4.30$ mm^{-1}.

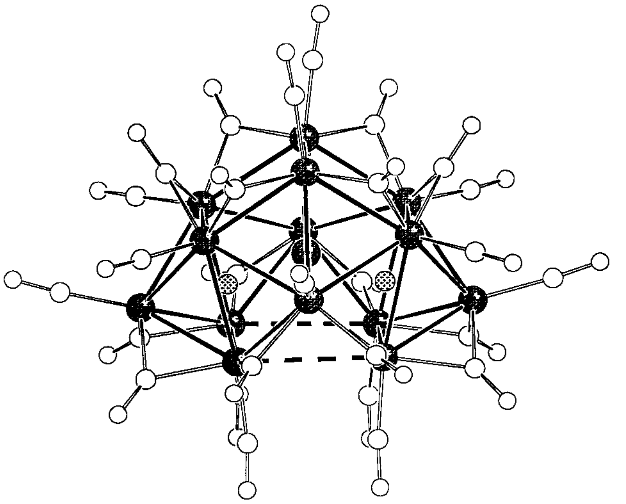

Figure 2. Structure of the $[Rh_{15}C_2(CO)_{28}]^-$ anion (C_2 precise and C_{2v} idealized symmetry, ref 9).

the principle of charge equalization, a driving force in determining the ligands' connectivity. As a matter of fact, while most metal atoms are three-connected to the ligands, Rh(4) remains two-connected and Rh(5) is four-connected, a situation never observed before in cluster compounds.

The $Rh_{15}C_2$ polyhedron, although of unusual geometry, is not an absolute novelty. Quite a few years ago we characterized the $[Rh_{15}C_2(CO)_{28}]^-$ anion,[9] which, despite its different chemical story, contains a strictly comparable metal atom cluster and, to a large extent, similar ligand distribution (Figure 2). The main difference between the $Rh_{15}C_2$ polyhedra resides in the lengths of the basal prism edges spanned by the iodide ligands in the trianion [2.927(1) Å] and unbridged and very stretched in the monoanion [3.332(3) Å]. Quite interestingly the ligands stereogeometry in the monoanion is that envisaged for the "symmetrized" trianion. The bridging iodide ligands replace four terminal CO groups of the monoanion so that the two species are isoelectronic.The Rh−Rh interactions, not surprisingly, are spread in a wide range [2.694−3.173(1), av 2.89 Å] because the molecular symmetry is C_1. Some average values of interest are as follows: Rh−Rh(CO-bridged) 2.80, Rh−Rh(unbridged) 2.97, Rh−Rh(core−surface) 2.88, Rh−Rh(I-bridged) 2.93, Rh−C(carbide) 2.06, Rh−I 2.68 Å. These values well compare to those found in the $[Rh_{15}C_2(CO)_{28}]^-$ anion:[9] Rh−Rh(overall) 2.88, Rh−Rh(CO-bridged) 2.81, Rh−Rh(unbridged) 2.93, Rh−Rh(core−surface) 2.90, Rh−C(carbide) 2.06 Å.

The stereochemical peculiarities exhibited by $[Rh_{15}C_2(CO)_{24}I_2]^{3-}$ can explain the disorder found in $[Rh_{15}C_2(CO)_{24}Br_2]^{3-}$. We have ascertained that the $Rh_{15}C_2Br_2$ core and 12 CO ligands conforming to the C_{2v} symmetry of the metal atom cluster (see above) are coincident with the diiodo species. The disorder affects the ligands of the dibromide corresponding to those arranged in chiral fashion in the diiodide. Our rationalization assumes that the dibromide is isostructural with the diiodide also in the blurred region and that the disorder is a packing effect. The well-behaved crystals of $[NEt_4]_3[Rh_{15}C_2(CO)_{24}I_2]$ contain the racemic mixture of the chiral anions orderly positioned in separate sites. The crystals of $[N(n\text{-}Pr)_4]_3[Rh_{15}C_2(CO)_{24}Br_2]$, on the contrary, contain anions of opposite chirality placed at random in their sites and, in addition, randomly rotated around the 2-fold axis. In this way an average C_2 symmetry is generated in the crystal and the ligands not conforming to that symmetry produce multiple images in the electron density map. The observed multiplicities of electron density peaks are in complete agreement with this model of disorder. It is now clear the reason we had not been able to disentangle the disorder: making "good" use of our experience in carbonyl cluster stereochemistry, we could neither imagine nor accept an unnecessarily asymmetric ligand geometry. Why then do the $[NEt_4]^+$ and $[N(n\text{-}Pr)_4]^+$ salts contain ordered and disordered isostructural anions, respectively? Very likely the smaller $[NEt_4]^+$ cation is quite sensitive to the surface features of the anion and is efficient in inducing its ordered crystallization. The bulkier $[N(n\text{-}Pr)_4]^+$ cation, on the other hand, packs more loosely and is unable to discriminate chirality and orientation of the counterion.

The ligands' geometry found in these anions can be assumed to persist in solution and allows a rationalization of their ^{13}C NMR spectra (see previous section). The fluxional ligands could be those adopting the chiral arrangement, while the static ones can be associated with the region conforming to C_{2v} symmetry (2 + 2 terminal and 4 + 3 (or perhaps 4?) bridging).

The molecular structures discussed above raise a question concerning the reason a chiral ligand coverage has been adopted even though it was not a geometrical necessity. We prefer to deal with the problem when the structures of all the $[Rh_{15}C_2(CO)_{24}X_2]^{3-}$ anions are elucidated. In the presence of the complete set of structures we hope to tell apart packing effects and true intramolecular features.

Experimental Section

All operations were carried out under nitrogen with a standard Schlenk-tube apparatus. Tetrahydrofuran was distilled from sodium benzophenone and propan-2-ol from aluminum isopropoxide. All other analytical grade solvents were degassed in a vacuum and stored under nitrogen. The compounds $[Rh(CO)_2(MeCN)_2]BF_4$[7] and $K_2[Rh_{12}C_2(CO)_{24}]$[4] were prepared by the published methods; the latter, obtained as a crude product with KCl impurity, was purified by extraction with thf and then vacuum-dried to give a black amorphous solid whose average formula was $K_2[Rh_{12}C_2(CO)_{24}]\cdot 2\text{-}4thf$. Infrared spectra were recorded on a Perkin-Elmer 16PC FT-IR spectrophotometer, using 0.1 mm CaF_2 cells previously purged with nitrogen. ^{13}C NMR spectra were recorded at 75.469 MHz with a resolution of ±0.85 Hz on a Bruker instrument.

Synthesis of Anion 1 as Potassium Salt and Metathesis with Bulky Cations. In a typical preparation $K_2[Rh_{12}C_2(CO)_{24}]\cdot 2-4(thf)$ (1087.0 mg, ca. 0.5 mmol) and $[Rh(CO)_2Cl]_2$ (230.2 mg, 0.60 mmol) were dissolved under nitrogen in thf (25 mL) and heated at 65−70 °C with stirring. When IR monitoring revealed (after ca. 5 h) the predominant presence of the anion **1** (ca. 2033 s, 1860 m, 1820 mw cm^{-1}), the solution was cooled at room temperature and filtered to remove some precipitate, which, before being discarded, was washed with thf (5 + 5 mL). The resulting clear solution with the collected washings was treated with *n*-hexane (50 mL) to give an oily precipitate. After decantation, the mother liquor was removed with a syringe and the residue redissolved with thf (10 mL) and reprecipitated with *n*-hexane (15 mL). The new mother liquor was removed and discarded, and the precipitate was finally washed with 10 mL of *n*-hexane, decanted, and vacuum-dried to yield ca. 850 mg of dry potassium salt. This same reaction can be performed as well using MeOH as a solvent, and also $[Rh(CO)_2Cl]_2$ may be replaced by an equimolecular amount of the less common $[Rh(CO)_2(MeCN)_2]BF_4$.

Several portions of a methanolic solution obtained by dissolution of the potassium salt (each containing ca. 50 mg in 2−3 mL) were carefully layered with a methanol or propan-2-ol solution (10 mL) containing 40−50 mg of one of the following cations as BF_4^- salts: $[NMe_4]^+$, $[NEt_4]^+$, $[NEt_3Bz]^+$, $[N(n\text{-}Pr)_4]^+$, $[N(n\text{-}Bu)_4]^+$, $[PPh_4]^+$, $[N(PPh_3)_2]^+$, or the crown ethers 18-c-6, 15-c-5, and dibenzo 18-c-6. When the diffusion of the solvents was complete (about a week), only the $[NEt_4]^+$, $[N(n\text{-}Pr)_4]^+$, and $[K(18\text{-}c\text{-}6)]^+$ salts showed the presence of a few very tiny crystals. Crystals of suitable size of the $[NEt_4]^+$ salt were tested for X-ray crystal analysis and gave no diffraction. Recrystallization of these samples and of the amorphous ones (from acetone with layering of propan-2-ol) did not improve the results but gave major decomposition of the samples, according to IR spectra.

Synthesis of $[Rh_{15}C_2(CO)_{24}X_2]^{3-}$ for X = Cl (2a), Br (2b), I (2c). The following method details the preparation of the bromo derivative 2b, but applies to the production of anions 2a and 2c as well. A methanolic solution containing the potassium salt of the anion 1, prepared according to the above-reported procedure (150−200 mg in 10 mL of MeOH), was treated dropwise with $[N(n\text{-}Pr)_4]Br$ (0.5 g in 20 mL of propan-2-ol). After addition of water to complete the precipitation, the precipitate was filtered and washed with some water (4 × 5 mL) and vacuum-dried. The product was redissolved with acetone (4 mL) and cautiously layered with propan-2-ol to yield within a few days a crystalline product. Yield: 70−80 mg (Found: C, 25.16; H, 2.66; N, 1.71. Calcd for $[N(n\text{-}Pr)_4]_3[Rh_{15}C_2(CO)_{24}Br_2]$: C, 25.17; H, 2.86; N, 1.42). The crystals obtained in this way were suitable for X-ray diffraction and allowed the determination of the crystal structure here reported.

The $[NMe_4]_3[Rh_{15}C_2(CO)_{24}Cl_2]$ salt was obtained in this way and with similar yield, using $[NMe_4]Cl$ (Found: C, 18.27; H, 1.48; N, 1.50. Calcd for $C_{38}H_{36}Cl_2N_3O_{24}Rh_{15}$: C, 18.02; H, 1.43; N, 1.66). Use of $[NMe_4]I$ or $[NEt_4]I$ analogously yields the anion $[Rh_{15}C_2(CO)_{24}I_2]^{3-}$ (**2c**), as the salt of the respective cation.

Synthesis of $[Rh_{15}C_2(CO)_{24}I_2]^{3-}$ (2c) from $Rh_4(CO)_{12}$ and I^-. $K_2[Rh_{12}C_2(CO)_{24}]\cdot 2\text{−}4(thf)$ (284 mg, ca.0.12 mmol), $Rh_4(CO)_{12}$ (93 mg, 0.12 mmol), and $[NEt_4]I$ (62 mg, 0.24 mmol) were placed in a Schlenk tube under N_2 atmosphere, and thf (10 mL) was added. The mixture was stirred and heated at 65 °C for 6−7 h, when the IR spectrum showed essentially the characteristic bands of the product at 2010 and 1839 cm^{-1} (Table 1). On cooling at room temperature, some impurities precipitated from the solution, together with a part of the product, which did not appear worth recovering. The clear thf solution obtained by filtration (ca. 8 mL) was layered with propan-2-ol (22 mL) to give after diffusion a partially crystalline precipitate. Recrystallization was made by dissolution in a 1:1 mixture of thf and acetone (4 mL), followed by layering of a 3-fold volume of propan-2-ol. When the diffusion of the solvents was complete (about a week), well-shaped black crystals containing a clathrated molecule of acetone were recovered. Estimated yield: ca. 150 mg (Found: C, 21.53; H, 2.30; N, 1.40. Calcd for $[NEt_4]_3[Rh_{15}C_2(CO)_{24}I_2]$.acetone: C, 21.63; H, 2.26; N, 1.43). The reported X-ray structural analysis and ^{13}C NMR spectrum were obtained from this sample.

A synthesis was performed similarly in acetone with $[NMe_4]I$, but the purification of the product was more difficult (Found: C, 15.93; H, 1.99; N, 1.47. Calcd for $[NMe_4]_3[Rh_{15}C_2(CO)_{24}I_2]$: C, 16.80; H, 1.34; N, 1.55).

The same procedure, using $[N(n\text{-}Pr)_4]Br$, was used to obtain $[N(n\text{-}Pr)_4]_3[Rh_{15}C_2(CO)_{24}Br_2]$.

Crystallography. The solid state structure of the anion $[Rh_{15}C_2(CO)_{24}I_2]^{3-}$ (**2c**) was determined in its $[NEt_4]^+$ salt by a diffraction experiment carried out on a Bruker SMART CCD diffractometer at room temperature. Cell parameters were refined from the observed omega angles of all the strong reflections. A highly redundant set of observations was measured for a complete diffraction sphere (θ_{max} = 28.3°). The collected frames were processed by SAINT sofware for integration; an absorption correction was applied together with merging (SADABS). The structure was solved by direct methods that showed a $Rh_{15}I_2$ core of heavy atoms in general position. Successive Fourier calculations revealed 24 CO ligands, 3 $[NEt_4]^+$ cations, and one molecule of acetone. The structure model was refined by full-matrix least-squares calculations on F^2 down to a conventional *R* factor 0.037 for 17 654 observed reflections. All the atoms in the anion and those not affected by disorder in the cations and solvent were assigned anisotropic thermal motion parameters. The hydrogen atoms were added in calculated positions and refined riding the pertinent carbon atoms [C−H = 0.97 Å]. The CH_2 groups in two $[NEt_4]^+$ cations were found partially disordered over two sites defining the vertexes of cubes centered at the N atoms. Occupancy factors of 0.80 and 0.55, respectively, were refined for their main images. The third cation exhibited unusually high thermal motion but did not show static disorder. After convergence no significant features were found in the difference electron density map, and residual peaks were in the range +0.98−0.65 e A^{-3}. The SHELX programs were used in all the calculations.[14] Crystal data and experimental details are reported in Table 3.

Table 3. Crystal Data and Experimental Details for $[NEt_4]_3[Rh_{15}C_2(CO)_{24}I_2]\cdot(CH_3)_2CO)$ (2c)

formula	$C_{50}H_{60}I_2N_3O_{24}Rh_{15}\cdot(CH_3)_2CO$
M	2942.50
temp, K	293(2)
wavelength, Å	0.71073
cryst symmetry	monoclinic
space group	$P2_1/n$ (No. 14)
a, Å	20.8365(2)
b, Å	15.0577(2)
c, Å	24.9047(3)
β, deg	93.693(1)
cell volume, $Å^3$	7797.6(2)
Z	4
D_c, Mg m^{-3}	2.478
μ(Mo Kα), mm^{-1}	3.94
F(000)	5465
cryst size, mm	0.35 × 0.40 × 0.45
θ limits, deg	2.13−28.29
no. of reflns collected	83916(±h, ±k, ±l)
no. of unique obsd reflns [$F_o > 4\sigma(F_o)$]	17 654 [R_{int} 0.0319]
goodness of fit on F^2	0.988
$R_1(F)^a$, $wR_2(F^2)^b$	0.0269, 0.0648
weighting scheme	$a = 0.0378$, $b = 0^b$
largest diff peak and hole, e $Å^{-3}$	1.01 and −0.75

[a] $R = \Sigma||F_o| - |F_c||/\Sigma|F_o|$. [b] $wR_2 = [\Sigma w(F_o^2 - F_c^2)^2/\Sigma w(F_o^2)^2]^{1/2}$ where $w = 1/[\sigma^2(F_o^2) + (aP)^2 + bP]$ where $P = (F_o^2 + 2F_c^2)/3$.

Acknowledgment. We thank Prof. Francesco Demartin (University of Milan) for his interest in this work and for allowing access to the Bruker SMART diffraction facilities. Financial support by MURST (COFIN98), CNR, and University of Bologna (Funds for Selected Research Topics) is also acknowledged.

Supporting Information Available: Tables of X-ray crystal data, final atomic coordinates, bond lengths and angles, anisotropic thermal parameters, and hydrogen atom coordinates for **2c**. This material is available free of charge via the Internet at http://pubs.acs.org.

OM000577P

---

[14] Sheldrick, G. M. *SHELXS 86*, Program for crystal structure solution; University of Gottingen, 1986. Sheldrick, G. M. *SHELXL 93*, Program for crystal structure refinement; University of Gottingen, 1993.